


# Single-frequency Brillouin lasing based on a birefringent fiber Fabry–Pérot cavity F

Cite as: Appl. Phys. Lett. **120**, 091102 (2022); <https://doi.org/10.1063/5.0079168>

Submitted: 18 November 2021 • Accepted: 22 January 2022 • Published Online: 28 February 2022

 Jian Guo,  Kunpeng Jia,  Xiaohan Wang, et al.

## COLLECTIONS

 This paper was selected as Featured



View Online



Export Citation



CrossMark

 QBLOX



1 qubit

Shorten Setup Time

**Auto-Calibration**

**More Qubits**

Fully-integrated

**Quantum Control Stacks**

**Ultrastable DC to 18.5 GHz**

Synchronized <<1 ns

Ultralow noise



100s qubits

[visit our website >](#)

# Single-frequency Brillouin lasing based on a birefringent fiber Fabry–Pérot cavity

Cite as: Appl. Phys. Lett. **120**, 091102 (2022); doi: [10.1063/5.0079168](https://doi.org/10.1063/5.0079168)

Submitted: 18 November 2021 · Accepted: 22 January 2022 ·

Published Online: 28 February 2022



View Online



Export Citation



CrossMark

Jian Guo,<sup>1</sup>  Kunpeng Jia,<sup>1,a)</sup>  Xiaohan Wang,<sup>1</sup>  Shu-Wei Huang,<sup>2</sup>  Gang Zhao,<sup>1</sup> Zhenda Xie,<sup>1,a)</sup>  and Shi-ning Zhu<sup>1</sup>

## AFFILIATIONS

<sup>1</sup>National Laboratory of Solid State Microstructures, School of Electronic Science and Engineering, College of Engineering and Applied Sciences, School of Physics, and Collaborative Innovation Center of Advanced Microstructures, Nanjing University, Nanjing 210093, China

<sup>2</sup>Department of Electrical, Computer and Energy Engineering, University of Colorado Boulder, Colorado 80309, USA

<sup>a)</sup>Authors to whom correspondence should be addressed: [jiakunpeng@nju.edu.cn](mailto:jiakunpeng@nju.edu.cn) and [xiezhenda@nju.edu.cn](mailto:xiezhenda@nju.edu.cn)

## ABSTRACT

Stimulated Brillouin scattering (SBS) in a high-Q resonator is capable for narrow-linewidth laser generation for various applications but is limited by on-resonance pump to SBS matching from single-longitudinal lasing. In this Letter, we present a narrow linewidth laser via SBS that is enhanced in a monolithic high-Q fiber resonator. The unique cross-polarization pump scheme based on fiber birefringence prevents high-order SBS and ensures single-frequency Brillouin lasing with high intracavity conversion efficiency. Fundamental linewidth of 50 Hz is achieved. Moreover, our scheme also allows precise characterization of Brillouin frequency shift and gain bandwidth of some nonlinear materials.

Published under an exclusive license by AIP Publishing. <https://doi.org/10.1063/5.0079168>

Narrow linewidth lasers with high coherence, low frequency noise, and high spectral purity are essential for both fundamental scientific studies and practical applications, such as frequency metrology, quantum sensing, atomic clocks, and microwave photonics.<sup>1–4</sup> Stimulated Brillouin laser (SBL) has a unique capability of narrowing the pump laser linewidth to produce a Stokes wave with lower fundamental linewidth.<sup>5–7</sup> Such linewidth narrowing effect can be further enhanced in a high-Q optical cavity as long as the SBL gain spectrum overlaps one cavity resonance. This cavity-enhanced SBL generation can be so efficient to achieve high pump depletion and results in higher SBL power than that of residue pump. However, in the normal cavity enhanced SBL configuration, frequencies of pump and SBL must be both precisely matched to that of the cavity resonances with the same polarization, within the narrow Brillouin gain bandwidth, which requires accurate control on cavity length. Moreover, the multi-longitudinal SBLs will be excited inevitably at high pump power due to the cavity enhancement between cavity modes and high-order SBL gain. The high-order SBLs will severely restrict the generation and application of SBL as a single-frequency laser.

Here, we study the SBL generation in a fiber Fabry–Pérot (FFP) resonator with a quality factor (Q) up to  $4.5 \times 10^7$ . The scheme of cross-polarization SBL generation is used, involving two orthogonally

polarized cavity modes of the FFP resonator. We utilize the stress-induced birefringence in optical fiber resulting from fiber mounting to detune the frequency offset between the two cavity modes with orthogonal polarizations. Such a scheme allows the deterministic single-frequency SBL generation in the FFP resonator with arbitrary cavity length in principle due to decoupling of the cavity length and frequency interval of resonances. Single-frequency SBL output power is measured to be 4.7 mW with a high intracavity conversion efficiency of 71%. The fundamental linewidth of 50 Hz is achieved, which is characterized by a short delay self-heterodyne interferometry (SDSHI) method.<sup>8</sup> The phase noise of the generated SBL is 20 dB lower than that of pump laser due to the noise reduction effect of the Brillouin process. Our scheme also provides an approach to characterize Brillouin-related properties in some nonlinear materials such as Brillouin frequency shift and gain spectrum profile.<sup>9,10</sup>

In previous works, whether the SBL generations were based on fiber ring cavities,<sup>11</sup> whispering gallery mode (WGM) resonators,<sup>12</sup> or Fabry Pérot (FP) resonators,<sup>13</sup> precise control of the cavity length is necessary to ensure that the Brillouin frequency shift is equal to integer multiples of the free spectral range of the resonator, as shown in Fig. 1(a). As a result, the generated SBL can cascade to high orders, thus preventing the SBL's applications as a single-frequency laser.<sup>14–18</sup> In

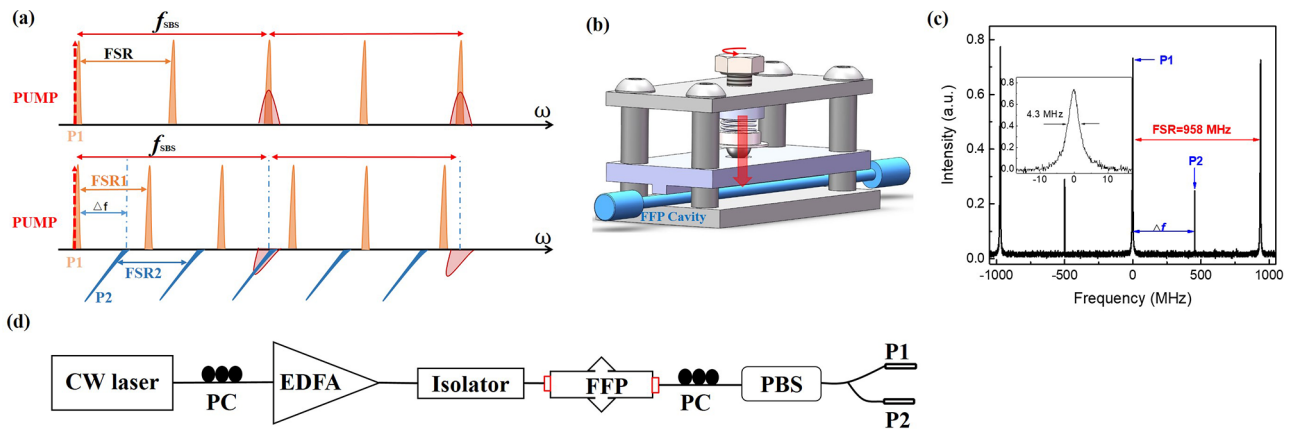


**FIG. 1.** (a) Schematic of our single-frequency Brillouin lasing in the FFP resonator (lower panel), in comparison to cascaded Brillouin lasing in previous resonators (upper panel). Our cross-polarization SBL generation scheme avoids frequency matching between cavity modes and Brillouin gain except the first order and allows frequency tuning within Brillouin gain spectrum by changing the stress-induced frequency offset  $\Delta f$  between two cross-polarization cavity modes. (b) Schematic of stress adjustment of optical fiber mount. (c) Transmission spectrum of the FFP resonator by sweeping a tunable laser across the resonances around 1550 nm. The free spectrum range (FSR) is measured to be 958 MHz. Inset, zoom-in view of one resonance whose Full width at half maximum (FWHM) is measured to be 4.3 MHz, corresponding to a Q of  $4.5 \times 10^7$ . (d) Schematic diagram of the experimental setup. PC, fiber polarization controller; EDFA, erbium doped fiber amplifier; FFP, fiber Fabry–Pérot resonator; PBS, polarizing beam splitter; P1 and P2, orthogonally polarized lasers (pump and SBL).

our scheme as shown in Fig. 1(b), we utilize the two orthogonally polarized mode families induced by the birefringence effect in the fiber resonator instead,<sup>19–22</sup> where the detuning of them can be finely tuned by adjusting the stress on the resonator. It is worth noting that stimulated Brillouin scattering (SBS) should be described as a nonlinear interaction among the acoustic, pump, and Stokes waves. For counter-propagating waves, if the pump and Stokes waves are linearly and orthogonally polarized in the polarization-maintaining fibers, the Brillouin gain will vanish. However, for a low-birefringence fiber, the Brillouin gain will not be zero even if the polarization of Stokes wave is orthogonal to the pump.<sup>19</sup> This is the key to generate the cross-polarization SBL. With pump laser and SBL gain spectrum aligned in resonances from orthogonally polarized mode families, efficient SBL can be generated, and most importantly, cascaded SBL is well-suppressed due to the mismatch of cavity resonances and high-order Brillouin gain spectra.

The FFP resonator we used in this paper is made of commercially available highly nonlinear fiber (HNLF) with a mode field diameter of 4.2  $\mu\text{m}$ . The techniques based on this fiber have the natural advantage of realizing high spectral-purity emission due to its mechanical stability, large effective optical mode area, and high nonlinear coefficient.<sup>23,24</sup> Both ends of the HNLF are mounted in commercial ceramic ferrules for the convenience of handling and plug-in coupling. Fine polishing and high-reflection dielectric coating ( $R > 99.5\%$  from 1530 to 1570 nm) on the two facets ensure a narrow resonance linewidth of 4.3 MHz, corresponding to a high Q of  $4.5 \times 10^7$ , characterized by sweeping the frequency of a tunable laser (Toptica CTL 1550) over the resonances, as shown in Fig. 1(c). The FSR is measured to be 958.3 MHz, matching well with the cavity length of 104 mm. The two orthogonal polarization mode families have a frequency offset of  $\Delta f$ , which are labeled as P1 and P2.

The schematic diagram of the experimental setup is shown in Fig. 1(d). We use an erbium-doped fiber amplifier (EDFA) as pump, which is seeded by a continuous-wave tunable laser with a linewidth of

about 5 kHz. A fiber polarization controller is used for optimizing the polarization of the pump to match one polarization axis of the FFP resonator. The single-mode fiber (SMF) from the isolator is low-loss spliced with a HNLF to optimize the plug-in coupling to the FFP resonator. The FFP resonator is mounted in a thermally conductive double-closure metal housing for precise temperature control, which integrates an adjustable stress controller used to change the birefringence of the FFP resonator, thus the frequency offset ( $\Delta f$ ) of two polarization mode families. The polarization controller is made of aluminum alloy by machining and has no electronic circuitry or power supply component. It includes a mechanical locking mechanism to keep the stress stable when it is tuned to a suitable position. So for the cavity, it adds no additional noise. The fiber polarization controller and polarizing beam splitter (PBS) after the FFP resonator are used to separate the orthogonally polarized residual pump laser and generated SBL. Subsequently, the output SBL is divided into two channels: one is for optical spectrum measurement and the other is combined with the pump laser to generate a beat signal for RF measurement.

For the SBL generation, the pump laser is tuned into a resonance around 1562 nm on the blue-detuned side. The pump laser can be thermo-locked on the blue side of the resonance.<sup>25</sup> The decrease in intensity or wavelength of the pump will reduce the cavity temperature, and the resonance will be blue-shifted closer to the pump to compensate for thermal dissipation, achieving a negative feedback mechanism, and vice versa. In this case, the resonator can overcome the power and frequency perturbation caused by the pump laser. By finely tuning the stress applied on the FFP, we can continuously change  $\Delta f$  to probe the gain spectrum of the cross-polarization stimulated Brillouin scattering. Once one of the cross-polarization resonances is close to the Brillouin gain spectrum centered at  $f_{SBS}$ , the beat signal between the SBL and the pump can be detected by a fast photodetector (EOT ET-5000F) and measured by an electric spectrum analyzer (ESA, Rohde & Schwarz FSV30), as shown in Figs. 2(a) and 2(b). The combination of the output spectrum and the clear single line in

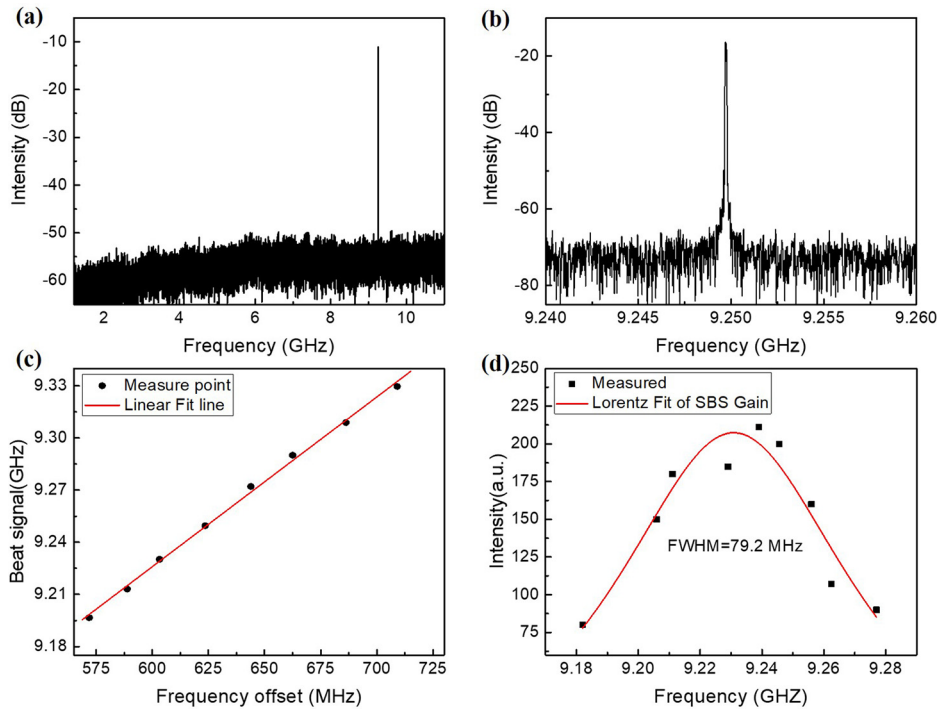


**FIG. 2.** Characterization of the generated single-frequency SBL. (a) RF measurement for the beat signal of pump and SBL. (b) Zoom-in view of the RF beat signal in (a), showing a clear single peak. (c) The frequency of the beat signal as a function of frequency offset between the two sets of cavity modes. (d) SBL intensity as a function of the Brillouin frequency shift. The Brillouin gain spectrum of HNLF is fitted with a Lorentzian function, and the FWHM is 79.2 MHz.

the RF spectrum indicates a single frequency SBL oscillation. The beat-note frequency changes linearly with  $\Delta f$  when the cross-polarization resonance sweeps over whole Brillouin gain spectrum, as shown in Fig. 2(c). We also record the transmitted SBL intensity as a function of the beatnote frequency, as shown in Fig. 2(d). Full width at half maximum (FWHM) of 79.2 MHz and center frequency of 9.249 GHz can be extracted from the Lorentz fitting, which match with the Brillouin gain bandwidth and frequency shift in highly nonlinear fiber, respectively.<sup>24,26</sup> The stress adjustment component in the experiment needs to be operated manually, which limits the modulation speed and accuracy of the SBL frequency. It can be further improved to be faster and more precise by utilizing piezo control techniques.

In the following study, the  $\Delta f$  is optimized for taking advantage of the maximum Brillouin gain. The threshold of SBL is measured to be 26 mW. With the increasing of pump power, the intracavity

conversion efficiency of SBL grows rapidly and reaches 71% with a pump power of 273 mW, according to the 3.9 dB intensity contrast on optical spectrum analyzer (OSA) spectra measured before PBS, as shown in Fig. 3(a). It is worth noting that even the pump power is as high as ten times the threshold, no higher-order Stokes wave is generated as we predicted. The output power of SBL as a function of that of the pump is shown in Fig. 3(b) with a slope conversion efficiency of 1.4%. We expect that the low total conversion efficiency is caused by the high-reflection dielectric coating.

The linewidth of the SBL in a high-Q resonator can be compressed by several orders of magnitude compared to the pump. The reason is that the narrow linewidth of the cavity resonance compared with the spectral width of the Brillouin gain allows suppressing the transmission of phase diffusion from pump to Stokes.<sup>27</sup> The theoretical fundamental linewidth of the SBL in the fiber is given by

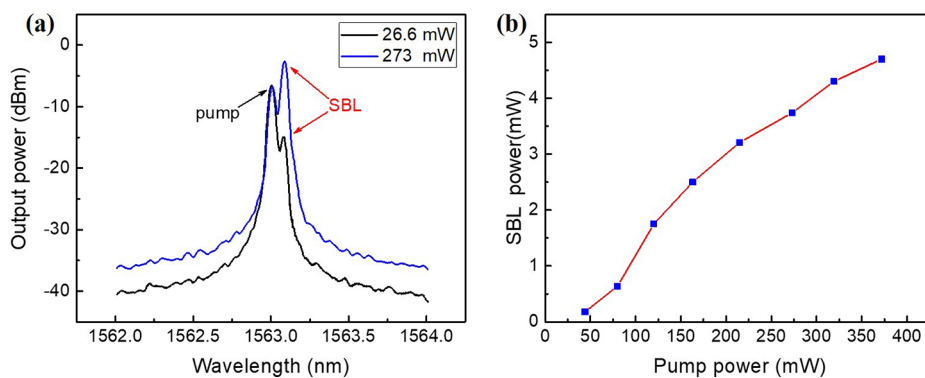


**FIG. 3.** (a) Output spectrum of the pump and SBL at a pump power of 26.6 and 273 mW, respectively. (b) SBL output power as a function of the pump power.

$$\Delta\nu_s = \frac{\Delta\nu_p}{(1 + \Gamma_A/\Gamma_C)^2}, \quad (1)$$

where  $\Gamma_A$ ,  $\Gamma_C$ ,  $\Delta\nu_p$ , and  $\Delta\nu_s$  represent the bandwidth of Brillouin gain, the linewidth of the FFP resonator, the linewidth of the pump and SBL, respectively. We assume  $\Gamma_A = 79.2$  MHz,  $\Gamma_C = 4.3$  MHz, and  $\Delta\nu_p = 5$  kHz, thus the linewidth of SBL is calculated to be 13.2 Hz with a linewidth reduction factor of 377 from pump laser. For such narrow linewidth laser, the conventional linewidth measurement methods like delayed self-heterodyne/homodyne interferometry<sup>28,29</sup> that require the fiber delay length to reach  $\sim 100$  km for a decoherence operation are obviously unpractical in experiment. To solve this problem, a new method for solving the numerical solution of ultra-narrow laser linewidth under the condition of insufficient delayed fiber length is proposed recently.<sup>8</sup> The contrast difference between the second peak and the second valley (CDSPT) of the strongly coherent envelope of the power spectrum measured from the short delay self-heterodyne interferometer (SDSHI) can be used as a basis for laser linewidth fitting for a given delayed fiber length.

Here, we characterize SBL linewidth by fitting the strong coherent envelope through self-coherent detection. The setup is shown in Fig. 4(a), consisting of an all-fiber unbalanced Mach-Zehnder interferometer with a 1 km delay fiber and a 40 MHz acousto-optic modulator (AOM). After amplified in an EDFA, the SBL is divided into two arms by a 50/50 fiber coupler.

The SBL in one arm goes through the optical fiber delay and the SBL in another arm goes through the AOM to produce a 40 MHz frequency shift. These two arms are recombined by another 50/50 fiber coupler. Their beating signal is then detected by a photodetector (PD) and measured using an ESA. Figs. 4(b) and 4(c) plot the measured results (red dot plots) and the fitting profiles (blue curve) obtained using the algorithm described in reference for the pump and SBL, respectively. The CDSPT of the SBL is 33 dB, corresponding to a linewidth of 50 Hz, which is 100 times narrower than the pump linewidth of 5 kHz. Compared with the theoretical linewidth of 13.2 Hz, we expect the test results to be limited by the noise caused by temperature and mechanical vibration.

The phase noise of the pump and SBL can be derived from the same SDSHI method with a 100 m delay length,<sup>30,31</sup> as shown in Fig. 4(e). The phase noise of SBL is strongly reduced from that of pump laser in the full measurement span. Above 10 kHz offset, the SBL phase noise is lower by  $\sim 20$  dBc/Hz compared with the pump phase noise. In the low-frequency regime, we analyze that the fluctuation of the SBL phase noise at the low-frequency regime is caused by the intensity noise of the EDFA and the acoustic vibration on the resonator. Nevertheless, comparing with the pump laser, the power spectral density (PSD) of SBL still has a certain suppression effect on phase noise in the low-frequency range. We expect that the phase noise can be further reduced by integrating the entire loop into a small package with better temperature and feedback control.<sup>32,33</sup>

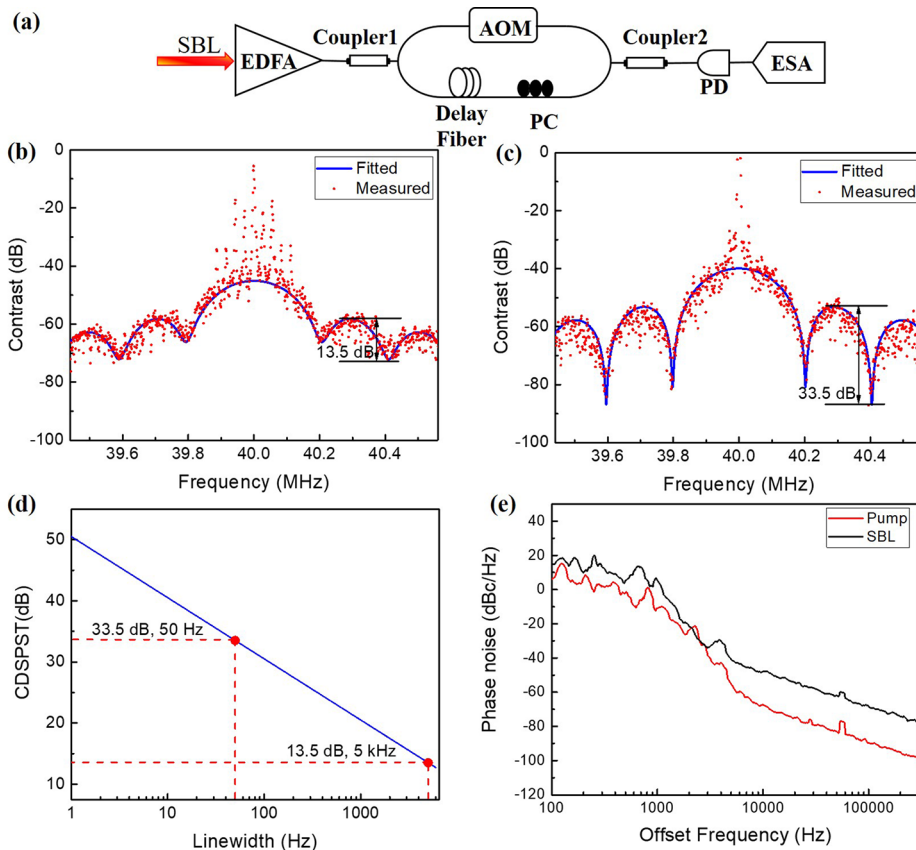


**FIG. 4.** Linewidth and phase noise measurement of pump and SBL. (a) Schematic diagram of the short delay self-heterodyne interferometer. AOM: acousto-optic modulator, PD: photodetector, ESA: electrical spectrum analyzer. (b) and (c) The self-heterodyne spectra of pump and SBL, with CDSPT of 13.5 and 33.5 dB, respectively. (d) Calculated CDSPT under 1 km delay fiber as a function of laser linewidth. The linewidths of pump and SBL can be extracted as 5 kHz and 50 Hz, respectively. (e) Phase noise performance of pump laser and SBL measured by the short delay self-heterodyne method with a 100 m delay length.

In conclusion, we have demonstrated a narrow linewidth stimulated Brillouin laser based on a fiber Fabry–Pérot resonator. Benefiting from the scheme of cross-polarization SBL generation, we overcome the limitation on the accuracy control of the cavity length and realize deterministic single-frequency SBL generation with the high-order Stokes emission perfectly suppressed. By tuning the frequency offset between the two sets of birefringence cavity mode, we estimated the Brillouin gain profile in HNLF. The SBL features a fundamental linewidth of 50 Hz, and the output power reaches milliwatt level, which is sufficient for many applications, such as high-resolution spectroscopy, distributed fiber sensing, and microwave photonics.<sup>34–36</sup> Lower threshold and narrower linewidth of SBL can be achieved by improving the Q of FFP, which is possible by optimizing the polishing and coating in the FFP fabrication process. The reduction of pump power requirement may also allow the direct pump by a simple laser diode. Thus, a compact and low-cost laser source with plug-play operation can be expected based on our unique FFP resonator, which is of special interest for many applications requiring field-deployable narrow-linewidth laser source.

This work was supported by the National Key Research and Development Program of China (Grant Nos. 2017YFB0405204, 2019YFA0705000, and 2017YFA0303700), the National Natural Science Foundation of China (Grant Nos. 51890861, 11690031, 11621091, and 11674169), Leading-edge technology Program of Jiangsu Natural Science Foundation (Grant No. BK20192001), Key R&D Program of Guangdong Province (Grant No. 2018B030329001), Excellent Research Program of Nanjing University (Grant No. ZYJH002), and Jiangsu Planned Projects for Postdoctoral Research Funds (Grant No. 2021K259B).

## AUTHOR DECLARATIONS

### Conflict of Interest

The authors have no conflicts to disclose.

### DATA AVAILABILITY

The data that support the findings of this study are available from the corresponding authors upon reasonable request.

## REFERENCES

- T. Udem, R. Holzwarth, and W. T. Hänsch, “Optical frequency metrology,” *Nature* **416**, 233 (2002).
- C. L. Degen, F. Reinhard, and P. Cappellaro, “Quantum sensing,” *Rev. Mod. Phys.* **89**, 035002 (2017).
- F. Riehle, “Optical atomic clocks and the quest for ultrastable lasers,” in *Frontiers in Optics*, edited by J. P. Delyett and D. Gauthier (Optical Society of America, Orlando, FL, 2013).
- D. Marpaung, J. Yao, and J. Capmany, “Integrated microwave photonics,” *Nat. Photonics* **13**, 80 (2019).
- S. P. Smith, F. Zarinetchi, and S. Ezekiel, “Narrow-linewidth stimulated Brillouin fiber laser and applications,” *Opt. Lett.* **16**, 393 (1991).
- W. Loh, J. Becker, D. C. Cole, A. Coillet, and S. A. Diddams, “A microrod-resonator Brillouin laser with 240 Hz absolute linewidth,” *New J. Phys.* **18**, 045001 (2016).
- G. D. Goodno and J. E. Rothenberg, “Suppression of stimulated Brillouin scattering in high power fibers using nonlinear phase demodulation,” *Opt. Express* **27**, 13129 (2019).
- S. Huang, Z. Tao, L. Min, and H. Wei, “Precise measurement of ultra-narrow laser linewidths using the strong coherent envelope,” *Sci. Rep.* **7**, 41988 (2017).
- T. R. Parker, “Temperature and strain dependence of the power level and frequency of spontaneous Brillouin scattering in optical fibers,” *Opt. Lett.* **22**, 787 (1997).
- M. Nikles, L. Thevenaz, and P. A. Robert, “Brillouin gain spectrum characterization in single-mode optical fibers,” *J. Lightwave Technol.* **15**, 1842 (1997).
- V. V. Spirin, J. Escobedo, D. A. Korobko, P. Mégret, and A. A. Fotiadi, “Dual-frequency laser comprising a single fiber ring cavity for self-injection locking of DFB laser diode and Brillouin lasing,” *Opt. Express* **28**, 37322 (2020).
- S. Grudinin, A. B. Matsko, and L. Maleki, “Brillouin Lasing with a CaF<sub>2</sub> whispering gallery mode resonator,” *Phys. Rev. Lett.* **102**, 43902 (2009).
- K. S. Abedin, “Single-frequency Brillouin lasing using single-mode As<sub>2</sub>Se<sub>3</sub> chalcogenide fiber,” *Opt. Express* **14**, 4037 (2006).
- J. Liu, Z. Li, P. Xiao, Q. Shen, and Z. Liang, “Optical generation of tunable microwave signal using cascaded Brillouin fiber lasers,” *IEEE Photonics Technol. Lett.* **24**, 22 (2012).
- M. Pang, S. Xie, X. Bao, D. P. Zhou, Y. Lu, and L. Chen, “Rayleigh scattering-assisted narrow linewidth Brillouin lasing in cascaded fiber,” *Opt. Lett.* **37**, 3129 (2012).
- M. Pang, X. Bao, and L. Chen, “Observation of narrow linewidth spikes in the coherent Brillouin random fiber laser,” *Opt. Lett.* **38**, 1866 (2013).
- T. Büttner, M. Merklein, I. V. Kabakova, D. D. Hudson, D. Y. Choi, B. Luther-Davies, S. J. Madden, and B. J. Eggleton, “Phase-locked, chip-based, cascaded stimulated Brillouin scattering,” *Optica* **1**, 311 (2014).
- N. Hayashi, Y. Mizuno, K. Nakamura, S. Y. Set, and S. Yamashita, “Fiber-optic cascaded forward Brillouin scattering seeded by backward stimulated Brillouin scattering,” in *CLEO: Science and Innovations*, 2018.
- P. Berceau, M. Fouché, R. Battesti, F. Bielsa, J. Mauchain, and C. Rizzo, “Dynamical behaviour of birefringent Fabry–Perot cavities,” *Appl. Phys. B* **100**, 803–809 (2010).
- A. Ejlli, F. Della Valle, and G. Zavattini, “Polarization dynamics of a birefringent Fabry–Perot cavity,” *Appl. Phys. B* **124**, 22 (2018).
- S. Garcia, F. Ferri, K. Ott, J. Reichel, and R. Long, “Dual-wavelength fiber Fabry–Perot cavities with engineered birefringence,” *Opt. Express* **26**, 22249–22263 (2018).
- M. Uphoff, M. Brekenfeld, G. Rempe, and S. Ritter, “Frequency splitting of polarization eigenmodes in microscopic Fabry–Perot cavities,” *New J. Phys.* **17**, 013053 (2015).
- M. O. van Deventer and A. J. Boot, “Polarization properties of stimulated Brillouin scattering in single-mode fibers,” *J. Lightwave Technol.* **12**, 585–590 (1994).
- D. Braje, L. Hollberg, and S. Diddams, “Brillouin-enhanced hyperparametric generation of an optical frequency comb in a monolithic highly nonlinear fiber cavity pumped by a cw laser,” *Phys. Rev. Lett.* **102**, 193902 (2009).
- T. Carmon, L. Yang, and K. J. Vahala, “Dynamical thermal behavior and thermal self-stability of microcavities,” *Opt. Express* **12**, 4742–4750 (2004).
- K. Jia, X. Wang, D. Kwon, J. Wang, and S. W. Huang, “Photonic flywheel in a monolithic fiber resonator,” *Phys. Rev. Lett.* **125**, 143902 (2020).
- A. Debut, S. Randoux, and J. Zemmouri, “Linewidth narrowing in Brillouin lasers: Theoretical analysis,” *Phys. Rev. A* **62**, 023803 (2000).
- Y. Li, Z. Fu, L. Zhu, J. Fang, H. Zhu, J. Zhong, P. Xu, X. Chen, J. Wang, and M. Zhan, “Laser frequency noise measurement using an envelope-ratio method based on a delayed self-heterodyne interferometer,” *Opt. Commun.* **435**, 244 (2019).
- R. O. Behunin, N. T. Otterstrom, P. T. Rakich, S. Gundavarapu, and D. J. Blumenthal, “Fundamental noise dynamics in cascaded-order Brillouin lasers,” *Phys. Rev. A* **98**, 23832 (2018).
- G. D. Domenico, S. Schilt, and P. Thomann, “Simple approach to the relation between laser frequency noise and laser line shape,” *Appl. Opt.* **49**, 4801–4807 (2010).
- D. Xu, F. Yang, D. Chen, F. Wei, H. W. Cai, Z. J. Fang, and R. H. Qu, “Laser phase and frequency noise measurement by Michelson interferometer composed of a 3 × 3 optical fiber coupler,” *Opt. Express* **23**, 22386–22393 (2015).
- V. V. Spirin, J. Escobedo, D. A. Korobko, P. Mégret, and A. A. Fotiadi, “Stabilizing DFB laser injection-locked to an external fiber-optic ring resonator,” *Opt. Express* **28**, 478 (2020).

- <sup>33</sup>S. Brian, X. Ji, D. Avik, and L. Michal, "Compact narrow-linewidth integrated laser based on a low-loss silicon nitride ring resonator," *Opt. Lett.* **42**, 4541 (2017).
- <sup>34</sup>H. Lee, T. Chen, J. Li, K. Y. Yang, S. Jeon, O. Painter, and K. J. Vahala, "Chemically etched ultrahigh-Q wedge-resonator on a silicon chip," *Nat. Photonics* **6**, 369 (2012).
- <sup>35</sup>N. T. Otterstrom, R. O. Behunin, E. A. Kittlaus, Z. Wang, and P. T. Rakich, "A silicon Brillouin laser," *Science* **360**, 1113 (2018).
- <sup>36</sup>S. Gundavarapu, G. M. Brodnik, M. Puckett, T. Huffman, and D. Blumenthal, "Sub-hertz fundamental linewidth photonic integrated Brillouin laser," *Nat. Photonics* **13**, 60 (2019).